Subscripts

c	at CP
g	gaseous phase
l	liquid phase
R	reduced property
v	change upon vaporization
$\bar{\rho}$	rectilinear diameter line, $(\rho_l + \rho_g)/2$
σ	coexistence property
1	single-phase property
2	two-phase property

Registry No. Ethylene, 74-85-1.

Literature Cited

(1) Douslin, D. R.; Harrison, R. H. *J. Chem. Thermodyn.* **1976**, *8*, 301.
(2) Harrison, R. H.; Douslin, D. R. *J. Chem. Eng. Data* **1977**, *22*, 24.
(3) Moldover, M. R. *J. Chem. Phys.* **1974**, *61*, 1766.
(4) Angus, S.; Armstrong, B.; de Reuck, K. M. "Ethylene, 1972"; Butterworths: London, 1972.
(5) Hastings, J. R.; Levelt Senger, J. M. H.; Balfour, F. W. *J. Chem. Thermodyn.* **1980**, *12*, 1009.
(6) Hastings, J. H.; Levelt Sengers, J. M. H. "Proceedings of the 7th Symposium on Thermophysical Properties"; American Society of Mechanical Engineers: New York, 1977; p 794.
(7) Nehzat, M. S. Ph.D. Dissertation, Texas A&M University, College Station, TX, 1978.
(8) Walton, C. W.; Mullins, J. C.; Holste, J. C.; Hall, K. R.; Eubank, P. T. *AIChE J.* **1978**, *24*, 1000.
(9) Hall, K. R.; Eubank, P. T. *Ind. Eng. Chem. Fundam.* **1976**, *15*, 80.
(10) Nehzat, M. S.; Hall, K. R.; Eubank, P. T. "Equations of State in Engineering and Research"; American Chemical Society: Washington, DC, 1979; Chapter 6.
(11) Yang, C. N.; Yang, C. P. *Phys. Rev. Lett.* **1964**, *13*, 303.
(12) Hall, K. R.; Eubank, P. T. *Ind. Eng. Chem. Fundam.* **1976**, *15*, 323.

Received for review October 1, 1981. Revised manuscript received July 28, 1982. Accepted January 20, 1983. Financial support of this project was by the National Science Foundation (ENG 76-00692).

Supplementary Material Available: The complete Table II containing the complete thermophysical properties of ethylene for isotherms ranging from 280.15 to 284.15 K at 0.2 K intervals for densities from 4.5 to 11.0 g-mol/dm^3 (21 pages). Table II of the manuscript is a sample for a single isotherm—the critical isotherm. Ordering information is given on any current masthead page.

Three-Phase Liquid–Liquid–Vapor Equilibria in the Methane + *n*-Pentane + *n*-Octane, Methane + *n*-Hexane + *n*-Octane, and Methane + *n*-Hexane + Carbon Dioxide Systems

Robert C. Merrill, Jr., Kraemer D. Luks,† and James P. Kohn*

Department of Chemical Engineering, University of Notre Dame, Notre Dame, Indiana 46556

The phase behavior of three ternary systems (methane + *n*-pentane + *n*-octane, methane + *n*-hexane + *n*-octane, methane + carbon dioxide + *n*-hexane) are presented for their region of L_1–L_2–V immiscibility. Liquid-phase compositions and molar volume data are presented as a function of temperature and pressure for the three-phase immiscibility region. The boundaries of the immiscibility regions are detailed. The methane + *n*-pentane + *n*-octane immiscibility is bounded by a locus of K points (L_1–L_2 = V), LCST points (L_1 = L_2–V), and Q points (S–L_1–L_2–V). The methane + *n*-hexane + *n*-octane immiscibility is bounded by a locus of K points, LCST points, and Q points and the L_1–L_2–V locus of the methane + *n*-hexane binary system. The methane + carbon dioxide + *n*-hexane immiscibility is bounded by a locus of K points and LCST points and by the L_1–L_2–V locus of the methane + *n*-hexane binary system. The L_1–L_2–V locus of the methane + *n*-hexane binary system is also presented.

Introduction

We are midway through an extensive study of liquid–liquid–vapor phenomena in liquefied natural gas systems. Earlier papers by Hottovy et al. (*1*, *2*) reported the phase behavior of the system methane + *n*-octane with the addition of a heavier solvent species. These heavier solvent species included ethane, propane, *n*-butane, and carbon dioxide. Hottovy showed that the addition of these species could induce L_1–L_2–V behavior in systems in which such behavior is not normally observed.

The three-phase regions studied by Hottovy were bounded by loci of K points (L_1–L_2 = V), LCST points (L_1 = L_2–V), and Q points (S–L_1–L_2–V), with a tricritical point at the point where the K-point and LCST-point loci intersect. Creek et al. (*3*) describe tricritical phenomena in systems containing methane and higher paraffins.

This paper presents the results for three new ternary systems which exhibit a region of immiscibility. These systems are methane + *n*-pentane + *n*-octane, methane + *n*-hexane + *n*-octane, and methane + carbon dioxide + *n*-hexane. The data presented herein include the compositions for the two liquid phases, and their molar volumes. The compositions and molar volumes for the bounding loci are also presented. The systems containing *n*-hexane are of great interest, because the methane + *n*-hexane binary forms its own L_1–L_2–V immiscibility locus. Data for the binary are presented and compared with earlier work by Lin et al. (*4*).

Experimental Section

This study employed apparatus previously used by Kohn and co-workers in other cryogenic studies (*5*). Earlier writings (*1*, *6*) have detailed the experimental procedure for L_1–L_2–V studies. For brevity's sake, the procedure will be only quickly sketched here.

All the phenomena were observed in a glass cell marked and calibrated for visual inspection. Stoichiometric and volumetric measurements were used to compute the compositions and molar volumes of each phase. A platinum resistance thermometer was used to measure the temperature of the system. This thermometer was calibrated to the 1968 IPTS scale and

† Present address: Department of Chemical Engineering, University of Tulsa, Tulsa, OK 74104.

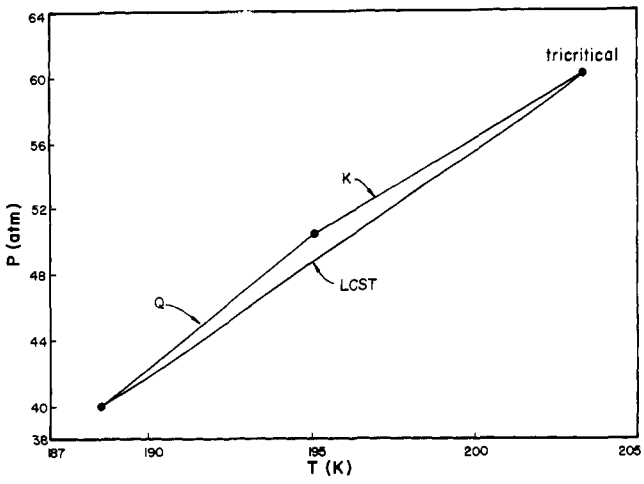

Figure 1. Boundaries of the L_1–L_2–V immiscibility region for the system methane + *n*-pentane + *n*-octane.

is estimated to be accurate to ±0.03 K. The pressure of the system was measured with a Heise Bourdon tube gauge, which was accurate to ±0.07 atm. The gauge was periodically checked against a dead-weight piston. The cell markings permitted the direct reading of the phase volumes to ±0.02 cm^3.

The gas phase was assumed to be essentially pure methane in the methane + *n*-pentane + *n*-octane and methane + *n*-hexane + *n*-octane systems, except at K points where the gas-phase compositions were calculated directly. This assumption was justified by the extremely low vapor-phase mole fractions of *n*-hexane and *n*-pentane in methane as reported in the literature (*4*, *10*). The gas-phase composition for the methane + carbon dioxide + *n*-hexane system was assumed to be composed of methane–carbon dioxide in their equilibrium ratio as reported by Mraw et al. (*7*). The compressibility of the gas phase was taken from NBS data for pure methane in the first two cases and was calculated by the Soave–Redlich–Kwong equation as modified by Graboski and Daubert (*8*, *9*) for the last case. The small errors inherent in these assumptions were further reduced by minimizing the amount of gas phase in the cell at all times.

The methane used in this study was Linde "Ultra Pure" grade with a stated purity of 99.97 mol %. The *n*-hexane and *n*-octane were both products of the Humphrey Chemical Co. with a stated purity of 99 mol %. The carbon dioxide was Matheson "Coleman Grade" with a stated purity of 99.99 mol %. The *n*-pentane used in the study was produced by Phillips Petroleum Co. with a stated purity of 99 mol %. The methane, *n*-pentane, *n*-hexane, and *n*-octane were used without further purification. The carbon dioxide was prepared by flashing it from the supply cylinder at room temperature to a storage cylinder at 273.15 K. The vapor phase was then vented to remove impurities.

The error is estimated to be such that the liquid-phase volumes are accurate to at least ±1.6%; solute composition in the L_1 phase is reliable to ±2%, and in the L_2 phase to ±8%. The second solvent compositions (*n*-pentane, *n*-hexane, carbon dioxide) are adjudged to be accurate to ±3.5%. These are very conservative estimates based on the limitations enumerated above.

Experimental Results

The results for the methane + *n*-pentane + *n*-octane system are presented in Tables I and II, those for methane + *n*-hexane + *n*-octane in Tables III and IV, , and those for methane + carbon dioxide + *n*-hexane in Tables V and VI. The immiscibility regions in *P*–*T* space are illustrated in Figures 1–3, respectively. The first table for each system presents the data for the L_2 phase (Tables I, III, and V), and the second gives the results for the L_1 phase (Tables II, IV, and VI). The

Table I. Raw Data for the *n*-Octane-Lean Liquid Phase L_2 of the System Methane + *n*-Pentane + *n*-Octane

temp, K	press., atm	mole fraction of *n*-pentane	mole fraction of *n*-octane	molar vol, mL/(g-mol)
		K (L_1-L_2 = V)		
196.95	52.60	0.0077	0.0018	83.6
196.97	52.60	0.0078	0.0019	87.2
197.73	53.08	0.0090	0.0027	87.6
200.61	57.05	0.01620	0.0011	86.8
200.71	57.08	0.01450	0.0019	70.1
		Q (S-L_1-L_2-V)		
191.86	44.81	0.0236	0.0044	64.0
192.15	45.93	0.0192	0.0027	69.4
192.83	46.37	0.0179	0.0035	64.7
193.22	47.43	0.0151	0.0023	63.2
		L_1-L_2-V		
190.00	41.93	0.0631	0.0091	59.6
192.00	44.93	0.0310	0.0045	66.7
192.00	45.05	0.0240	0.0075	65.4
192.00	45.21	0.0252	0.0048	67.4
194.00	47.84	0.0191	0.0066	65.6
194.00	47.94	0.0174	0.0052	65.9
194.00	48.01	0.0165	0.0050	66.7
194.00	48.51	0.0132	0.0033	63.8
194.00	48.58	0.0135	0.0029	67.4
194.00	48.65	0.0113	0.0026	65.7
194.00	48.72	0.0122	0.0034	69.4
196.00	50.69	0.0154	0.0056	70.7
196.00	50.89	0.0140	0.0043	75.3
196.00	51.23	0.0099	0.0028	70.5
196.00	51.37	0.0084	0.0022	71.9
196.00	51.44	0.0079	0.0020	71.4
198.00	53.14	0.0366	0.0020	63.6
198.00	53.28	0.0248	0.0014	69.9
198.00	53.47	0.0151	0.0009	80.3
200.00	55.75	0.0399	0.0020	61.2
200.00	55.81	0.0339	0.0020	64.1
200.00	55.89	0.0332	0.0013	62.7
200.00	55.96	0.0306	0.0016	68.0

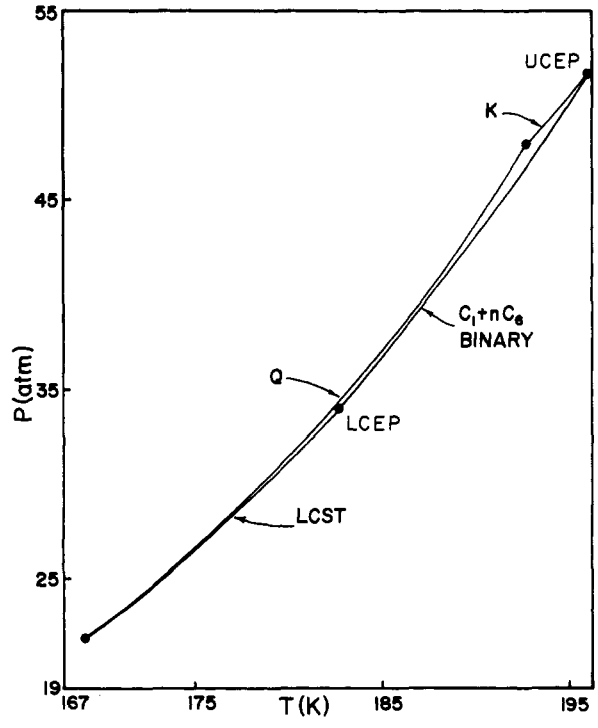

Figure 2. Immiscibility boundaries of the system methane + *n*-hexane + *n*-octane.

Table II. Raw Data for the *n*-Octane-Rich Liquid Phase L_1 of the System Methane + *n*-Pentane + *n*-Octane

temp, K	press., atm	mole fraction of *n*-pentane	mole fraction of *n*-octane	molar vol, mL/(g-mol)
		K (L_1-L_2 = V)		
195.95	51.44	0.176	0.137	70.0
196.31	51.85	0.220	0.113	58.2
196.67	52.33	0.189	0.114	70.0
199.84	49.34	0.172	0.031	65.0
200.35	56.84	0.104	0.015	76.8
201.28	58.41	0.135	0.014	62.4
		Q (S-L_1-L_2-V)		
189.32	41.71	0.163	0.081	63.7
190.75	43.62	0.169	0.104	65.6
191.79	45.11	0.185	0.096	50.6
		LCST (L_1 = L_2-V)		
193.58	46.97	0.100	0.018	58.5
193.75	47.10	0.104	0.019	58.6
196.09	50.12	0.090	0.013	59.9
196.25	50.41	0.093	0.014	60.2
197.90	52.72	0.091	0.010	58.8
199.22	54.55	0.079	0.007	60.4
199.54	55.07	0.086	0.008	60.3
		L_1-L_2-V		
190.00	42.27	0.153	0.058	60.6
190.00	42.37	0.163	0.071	62.8
192.00	44.89	0.162	0.061	61.7
192.00	44.97	0.170	0.074	63.9
192.00	45.25	0.180	0.109	68.5
192.00	45.39	0.193	0.096	67.4
192.00	45.45	0.199	0.103	54.0
194.00	47.43	0.175	0.061	63.3
194.00	47.64	0.169	0.064	62.0
194.00	47.82	0.174	0.076	65.2
194.00	47.97	0.176	0.107	66.3
194.00	48.31	0.180	0.090	65.7
194.00	48.38	0.202	0.105	54.4
194.00	48.38	0.229	0.118	60.7
196.00	49.92	0.130	0.024	60.0
196.00	50.12	0.130	0.023	58.9
196.00	50.56	0.176	0.061	63.2
196.00	50.64	0.176	0.067	62.8
196.00	50.83	0.181	0.079	64.6
196.00	51.17	0.183	0.091	65.6
196.00	51.37	0.225	0.116	59.6
198.00	53.07	0.147	0.028	59.7
198.00	53.69	0.181	0.063	62.8
198.00	53.89	0.179	0.068	61.5
200.00	55.78	0.104	0.0133	58.9
200.00	55.99	0.121	0.014	54.2
200.00	56.31	0.129	0.015	59.4

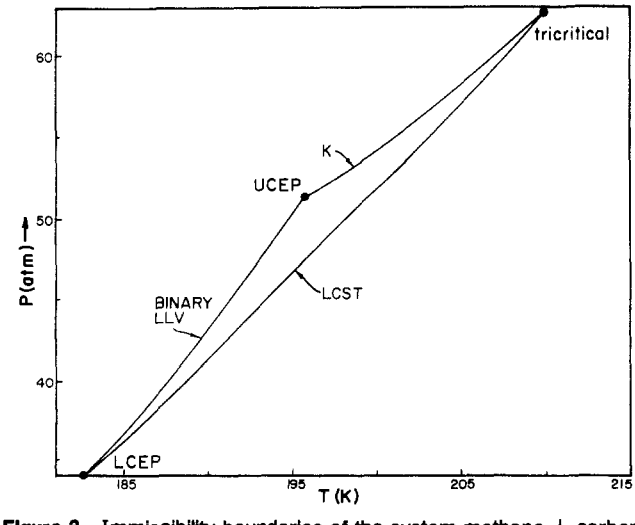

Figure 3. Immiscibility boundaries of the system methane + carbon dioxide + *n*-hexane.

Table III. Raw Data for the *n*-Octane-Lean Liquid Phase L_2 of the System Methane + *n*-Hexane + *n*-Octane

temp, K	press., atm	mole fraction of *n*-hexane	mole fraction of *n*-octane	molar vol, mL/(g-mol)
		K (L_1-L_2 = V)		
193.15	48.28	0.0054	0.0034	114.9
193.20	48.44	0.0	0.0156	88.7
193.69	48.96	0.0017	0.0012	90.2
193.85	48.94	0.0017	0.0021	99.0
194.14	49.37	0.0098	0.0018	81.04
194.29	49.63	0.0051	0.0013	91.3
		Q (S-L_1-L_2-V)		
181.38	32.76	0.0349	0.0053	58.0
181.92	33.38	0.0331	0.0046	57.9
182.61	34.20	0.0292	0.0042	57.40
182.20	36.16	0.0185	0.0067	52.44
187.62	40.59	0.0134	0.0030	62.3
191.94	46.29	0.0068	0.0029	71.2
192.00	46.65	0.0059	0.0021	72.2
192.20	46.56	0.0075	0.0036	71.5
		L_1-L_2-V		
182.00	33.38	0.0347	0.0034	55.6
182.00	33.38	0.0335	0.0033	55.0
182.00	33.44	0.0397	0.0019	57.92
182.00	33.44	0.0437	0.0037	58.0
182.00	33.45	0.0313	0.0039	61.5
182.00	33.51	0.0330	0.0039	60.8
182.00	33.64	0.0478	0.0022	63.9
180.00	31.33	0.0429	0.0053	54.0
180.00	31.33	0.0405	0.0050	55.6
180.00	31.40	0.0505	0.0040	53.7
178.00	29.28	0.0798	0.0038	54.5
178 00	29.29	0.0449	0.0056	54.0
184.00	35.55	0.0479	0.0036	59.9
184.00	35.62	0.0317	0.0043	56.8
184.00	35.62	0.0395	0.0035	59.8
184.00	35.62	0.0396	0.0031	57.6
184.00	35.69	0.0250	0.0069	57.0
184.00	35.69	0.0278	0.0090	59.6
184.00	35.69	0.0359	0.0055	59.7
184.00	35.76	0.0340	0.0034	57.7
184.00	35.82	0.0379	0.0030	61.7
184.00	35.96	0.0261	0.0042	59.9
186.00	37.87	0.0280	0.0036	57.5
186.00	37.93	0.0335	0.0022	57.8
186.00	38.00	0.0343	0.0006	58.5
186.00	38.00	0.0291	0.0022	58.0
186.00	38.07	0.0312	0.0021	58.1
186.00	38.14	0.0219	0.0025	58.1
186.00	38.20	0.0239	0.0027	59.7
186.00	38 20	0.0307	0.0011	59.4
186.00	38.21	0.0334	0.0006	59.2
188.00	40.31	0.0213	0.0037	61.0
188.00	40.31	0.0286	0.0022	58.82
188.00	40.52	0.0259	0.0027	59.4
188.00	40.58	0.0274	0.0020	58.8
188.00	40.59	0.0191	0.0062	59.9
188.00	40.59	0.0287	0.0022	59.7
188.00	40.72	0.0281	0.0019	59.7
188.00	40.93	0.0119	0.0037	61.6
190.00	42.90	0.0255	0.0018	60.7
190.00	42.90	0.0249	0.0018	60.8
190.00	43.17	0.0188	0.0016	63.0
190.00	43.17	0.0234	0.0016	61.6
190.00	43.17	0.0245	0.0017	63.4
190.00	43.52	0.0108	0.0021	63.9
192.00	45.96	0.0199	0.0013	65.4
192.00	46.23	0.0123	0.0037	76.1
192.00	46.30	0.0089	0.0025	71.7
192.00	46.36	0.0046	0.0038	71.5
192.00	46.58	0.0050	0.0027	73.6
194.00	48.68	0.0149	0.0001	70.0
194.00	49.09	0.0074	0.0034	72.3
194.00	49.16	0.0039	0.0011	77.2

Table IV. Raw Data for the *n*-Octane-Rich Liquid Phase L_1 of the System Methane + *n*-Hexane + *n*-Octane

temp; K	press., atm	mole fraction of *n*-hexane	mole fraction of *n*-octane	molar vol, mL/(g-mol)
		K (L_1-L_2 = V)		
193.06	48.21	0.2450	0.2008	94.5
193.35	48.49	0.2554	0.1446	84.2
193.56	49.00	0.2045	0.1387	73.4
193.76	49.06	0.2288	0.1297	77.2
194.24	49.53	0.2711	0.0201	71.8
194.86	50.24	0.2119	0.0390	56.7
195.02	50.31	0.2537	0.0103	64.9
		Q (S-L_1-L_2-V)		
174.48	25.88	0.1819	0.0261	59.7
175.16	26.49	0.1752	0.0265	57.4
176.62	27.99	0.1997	0.0371	62.6
184.80	36.36	0.2467	0.0898	76.7
189.96	43.82	0.2042	0.1368	72.1
190.51	44.60	0.2126	0.1427	75.2
191.91	46.81	0.2206	0.1786	84.4
192.36	47.14	0.2333	0.1977	90.4
		LCST (L_1 = L_2-V)		
174.69	26.23	0.1247	0.0097	56.7
174.84	26.17	0.1507	0.0087	56.41
175.94	27.25	0.1557	0.0121	58.3
177.14	28.39	0.0999	0.0056	55.05
177.81	28.88	0.1505	0.0087	56.9
178.29	29.48	0.1292	0.0063	56.4
178.43	29.62	0.1411	0.0068	57.1
179.02	29.16	0.1547	0.0089	57.5
		binary LCST		
182.91	34.18	0.1592	0.0	59.8
		L_1-L_2-V		
176.00	27.19	0.1587	0.0138	56.6
176.00	27.31	0.1944	0.0264	61.9
178.00	29.02	0.1491	0.0083	56.6
178.00	29.16	0.1757	0.0154	58.9
178.00	29.21	0.1959	0.0270	61.4
178.00	29.28	0.2014	0.0379	62.7
178.00	29.28	0.1555	0.0087	58.5
178.00	29.29	0.1777	0.0139	59.5
180.00	31.14	0.1881	0.0165	59.8
180.00	31.26	0.2040	0.0384	62.3
180.00	31.26	0.2053	0.0278	61.3
180.00	31.33	0.1770	0.0088	58.7
180.00	31.33	0.1902	0.0147	59.9
180.00	31.40	0.1821	0.0103	58.8
180.00	31.46	0.1861	0.0098	58.7
182.00	33.23	0.2277	0.0313	67.8
182.00	33.24	0.2033	0.0117	59.3
182.00	33.25	0.2105	0.0184	63.6
182.00	33.37	0.2276	0.0434	68.8
182.00	33.44	0.2202	0.0171	66.5
184.00	35.54	0.2451	0.0333	70.4
184.00	35.68	0.2488	0.0465	72.7
184.00	35.69	0.2176	0.0125	64.2
184.00	35.75	0.2232	0.0113	65.5
184.00	35.76	0.2276	0.0198	65.8
184.00	35.96	0.2415	0.0188	70.2
184.00	36.02	0.2414	0.0188	69.9
186.00	37.77	0.2232	0.0128	63.7
186.00	37.81	0.2022	0.0173	56.0
186.00	37.92	0.2392	0.0326	67.4
186.00	38.06	0.2375	0.0446	68.0
186.00	38.07	0.2256	0.0114	64.4
186.00	38.13	0.2380	0.0881	74.2
186.00	38.20	0.2379	0.0185	67.1
186.00	38.20	0.2478	0.0847	75.3
188.00	40.25	0.2508	0.0184	57.8
188.00	40.32	0.2320	0.0202	64.1
188.00	40.38	0.2670	0.0359	74.1
188.00	40.44	0.2349	0.0441	66.4
188.00	40.52	0.2363	0.0237	64.9
188.00	40.52	0.2391	0.0186	65.8
188.00	40.65	0.2402	0.0263	66.1
188.00	40.65	0.2378	0.0279	61.3
188.00	40.72	0.2390	0.0220	65.5
188.00	40.75	0.2301	0.0132	63.4
190.00	42.83	0.2354	0.0135	63.1
190.00	42.90	0.2431	0.0224	65.3
190.00	42.91	0.2384	0.0208	64.3
190.00	42.97	0.2437	0.0348	66.5
190.00	43.17	0.2433	0.0244	65.4
190.00	43.17	0.2445	0.0268	65.9
190.00	43.17	0.2451	0.0247	65.7
190.00	43.17	0.2376	0.0444	66.2
190.00	43.23	0.2271	0.0826	69.0
190.00	43.30	0.2318	0.0793	69.6
192.00	45.93	0.2754	0.0236	71.5
192.00	45.96	0.2605	0.0485	71.1
192.00	45.96	0.2685	0.0383	72.2
192.00	46.09	0.2793	0.0260	74.1
192.00	46.16	0.2898	0.1047	87.1
194.00	48.62	0.2634	0.0243	67.9
194.00	48.69	0.2593	0.0370	68.4
194.00	48.81	0.2586	0.0221	65.7
194.00	48.95	0.2452	0.0453	65.9
194.00	49.05	0.2753	0.0224	70.1

data for the binary system methane + *n*-hexane are presented in Table VII.

The region of L_1–L_2 immiscibility for the methane + *n*-pentane + *n*-octane system (Figure 1) is quite similar to those reported in Hottovy's work. This region is three-sided, bounded by loci of K points (L_1–L_2 = V), LCST points (L_1 = L_2–V), and Q points (S–L_1–L_2–V). Hottovy noticed that the region of immiscibility shifts toward lower temperatures and pressures as the second solvent increases in molecular weight. This trend is confirmed by the methane + *n*-pentane + *n*-octane system, which lies closer to the pure-methane vapor-pressure curve than any other three-sided region of immiscibility.

This progression ceases when *n*-hexane is the second solvent. This occurs because the methane + *n*-hexane system forms a binary L_1–L_2–V immiscibility in the region of the methane + *n*-hexane + *n*-octane ternary immiscibility. This binary immiscibility "cuts through" the expected three-sided immiscibility region. The resultant four-sided figure is bounded by K points, Q points, LCST points, and the binary immiscibility. The ternary's loci of K points and LCST points intersect the binary locus at its upper and lower critical end points (UCEP, LCEP), respectively. The immiscibility region is very narrow in pressure–temperature space, due to the similarity between *n*-hexane and *n*-octane. Indeed, this system might be considered to be mimicking the binary methane + *n*-hexane system (i.e., a quasi-binary in the spirit of Creek (*3*).

The binary methane + *n*-hexane immiscibility similarly forms one side of the methane + carbon dioxide + *n*-hexane system's region of immiscibility. However, carbon dioxide extends the L_1–L_2–V region to higher temperatures rather than lower as was the case for *n*-octane. There is no Q-point locus for this system; the binary locus forms the lower bound. The K-point and LCST-point loci intersect the binary's UCEP and LCEP. These critical loci also intersect each other at a tricritical point.

Data for the methane + *n*-hexane binary in this temperature range have been previously reported by Lin et al. (*4*). The binary measurements were repeated in this laboratory to provide both internal consistency and a check on the reasonableness of our reported data. Our data compare favorably with those of Lin and are shown in Table VII. Lin reported the K-point and LCST-point existence at 195.91 K, 51.37 atm and 182.46 K, 33.70 atm, respectively. The K point and LCST point elucidated in this study occurred at 195.72 K, 51.33 atm and 182.73 K, 34.05 atm, respectively. The difference between

Table V. Raw Data for the *n*-Hexane-Lean Liquid Phase L_2 of the System Methane + Carbon Dioxide + *n*-Hexane

temp, K	press., atm	mole fraction of *n*-hexane	mole fraction of CO_2	molar vol, mL/(g-mol)
		L_1-L_2-V		
204.00	57.46	0.0331	0.0841	64.0
204.00	57.96	0.0304	0.0850	66.2
202.00	55.96	0.0214	0.0083	60.7
200.00	53.45	0.0310	0.0783	63.7
200.00	53.65	0.0299	0.0751	68.9
198.00	50.93	0.0371	0.0791	59.8
198.00	52.02	0.0233	0.0404	65.9
198.00	52.49	0.0209	0.0267	68.3
196.00	49.09	0.0323	0.0436	61.0
196.00	49.30	0.0284	0.0394	62.2
196.00	49.36	0.0285	0.0259	63.3
196.00	49.36	0.0303	0.0263	62.9
196.00	49.43	0.0256	0.0267	62.5
196.00	50.38	0.0204	0.0181	66.8
196.00	50.44	0.0182	0.0251	61.1
196.00	50.59	0.0206	0.0188	67.0
196.00	50.66	0.0159	0.0029	63.8
196.00	51.00	0.0178	0.0022	69.2
194.00	46.17	0.0437	0.0283	59.6
194.00	46.44	0.0397	0.0400	59.0
194.00	47.52	0.0292	0.0238	61.3
194.00	47.73	0.0210	0.0046	64.7
194.00	47.80	0.0246	0.0012	64.0
194.00	47.87	0.0274	0.0000	63.9
192.00	43.85	0.0551	0.0305	58.04
192.00	44.67	0.0374	0.0124	59.4
192.00	44.87	0.0266	0.0047	60.9
192.00	45.15	0.0361	0.0134	61.8
192.00	45.49	0.0291	0.0031	61.2
190.00	42.22	0.0466	0.0139	57.8
190.00	42.43	0.0387	0.0032	58.7
190.00	42.56	0.0411	0.0101	60.3
190.00	42.70	0.0361	0.0035	63.4
188.00	39.37	0.0623	0.0143	56.3
188.00	39.77	0.0468	0.0042	57.0
188.00	39.91	0.0473	0.0039	57.3
188.00	40.11	0.0455	0.0035	56.9
186.00	37.60	0.0592	0.0035	55.7
		K (L_1-L_2 = V)		
197.15	52.09	0.0055	0.0014	100.57
199.80	54.26	0.0090	0.0255	88.97
200.05	55.35	0.0078	0.0392	86.62
200.18	54.53	0.0073	0.0234	93.10
200.19	54.33	0.0044	0.0194	98.07
201.83	55.96	0.0080	0.0364	89.74
202.33	56.37	0.0104	0.0522	83.86
202.91	56.85	0.0149	0.0628	105.84
203.98	57.86	0.0137	0.0747	78.24

measured *n*-hexane compositions in the *n*-hexane-lean phase averaged 0.61% for L_1–L_2–V points and was 0.23% for the K point and 3.64% for the LCST. (Difference is defined here as (Lin value − this value)/(this value).) For the *n*-hexane-rich phase this difference averaged −1.84% for L_1–L_2–V points and was −6.51% for the K point. The pressures agreed to an average of 0.75%. The discrepencies between Lin's data and this work can undoubtedly be ascribed to the differences in purities in the materials used. These effects, of course, would be magnified in the critical regions due to the "flatness" of the *T*–*x* curve.

Glossary

C	critical point
K	the K point or critical end point of an L_1–L_2–V region occurs when L_2 = V in the presence of L_1
L_1	liquid phase rich in solute
L_2	liquid phase lean in solute
LCST	lower critical solution temperature, this occurs when L_1 and L_2 are critical with each other

Table VI. Raw Data for the *n*-Hexane-Rich Liquid Phase L_1 of the System Methane + Carbon Dioxide + *n*-Hexane

temp, K	press., atm	mole fraction of *n*-hexane	mole fraction of CO_2	molar vol, mL/(g-mol)
		LCST (L_1 = L_2-V)		
184.14	35.41	0.1305	0.0157	56.26
184.76	35.96	0.1495	0.0176	56.72
189.61	41.13	0.1566	0.0310	57.98
189.85	41.39	0.1698	0.0260	58.92
190.69	42.36	0.1701	0.0252	59.32
191.13	42.90	0.1707	0.0338	58.65
193.74	45.36	0.1306	0.0454	58.31
199.18	51.82	0.1408	0.0743	58.90
199.34	51.75	0.1251	0.0674	58.27
202.63	55.70	0.1161	0.0901	59.15
188.41	39.50	0.1141	0.0310	56.60
191.17	42.49	0.0850	0.0323	57.36
		K (L_1-L_2 = V)		
196.89	52.22	0.2365	0.0123	60.71
197.76	52.28	0.2304	0.0344	63.22
197.92	52.42	0.2232	0.0428	62.80
198.10	52.89	0.2264	0.0334	61.29
198.13	52.90	0.2334	0.0079	64.76
199.87	54.27	0.2035	0.0883	62.84
203.24	57.06	0.1423	0.1380	56.89
203.66	57.67	0.1482	0.0848	59.03
		L_1-L_2-V		
204.00	58.07	0.1152	0.1078	58.5
204.00	58.21	0.1184	0.1018	59.2
202.00	55.16	0.1302	0.0807	59.5
202.00	55.36	0.1261	0.1226	55.4
202.00	55.43	0.1364	0.0938	57.4
202.00	55.63	0.1548	0.0664	59.5
200.00	52.70	0.1345	0.0774	59.0
198.00	51.21	0.1778	0.0609	59.0
198.00	51.34	0.1740	0.0599	58.1
198.00	52.08	0.2135	0.0000	65.1
198.00	52.42	0.2079	0.0429	60.1
198.00	52.68	0.2332	0.0214	64.1
196.00	48.49	0.1626	0.0659	59.2
196.00	49.49	0.1980	0.0419	60.6
196.00	49.96	0.2179	0.0278	61.6
196.00	50.04	0.2074	0.0353	60.5
196.00	50.17	0.2171	0.0279	61.3
196.00	50.38	0.2285	0.0312	65.7
196.00	50.65	0.2313	0.0017	61.0
196.00	50.73	0.2322	0.0171	61.5
194.00	46.30	0.1820	0.0398	59.9
194.00	46.83	0.2063	0.0293	61.1
194.00	46.91	0.2004	0.0377	60.5
194.00	46.97	0.2098	0.0322	64.0
194.00	46.99	0.2030	0.0286	61.3
194.00	47.04	0.2120	0.0317	64.4
194.00	47.46	0.2151	0.0240	62.2
194.00	47.74	0.2218	0.0172	60.8
192.00	44.12	0.1595	0.0330	59.5
192.00	44.20	0.1845	0.0250	60.5
192.00	44.25	0.1905	0.0277	60.1
192.00	44.25	0.1951	0.0291	63.5
192.00	44.27	0.1847	0.0256	60.3
192.00	44.32	0.1918	0.0294	62.4
192.00	44.80	0.2136	0.0075	61.4
192.00	44.95	0.2083	0.0187	60.1
192.00	45.19	0.2166	0.0185	60.3
190.00	41.61	0.1623	0.0244	59.2
190.00	42.23	0.1936	0.0184	59.6
190.00	42.56	0.2044	0.0204	58.8
188.00	39.83	0.1927	0.0228	58.9
188.00	39.83	0.1934	0.0245	58.6
188.00	39.90	0.1983	0.0092	59.6
186.00	37.32	0.1645	0.0059	58.2
186.00	37.45	0.1534	0.0188	57.3
186.00	37.52	0.1690	0.0203	57.5

Table VII. Experimental Data for the Methane + n-Hexane Binary[a]

temp, K	press., atm	mole fraction of n-hexane L_1	mole fraction of n-hexane L_2	molar vol, mL/(g-mol) L_1	molar vol, mL/(g-mol) L_2
		K (L_1-L_2 = V)			
195.72	51.33	0.2323	0.0117	57.82	153.86
		L_1-L_2-V			
194.00	48.67	0.2525	0.0179	63.89	67.36
192.00	45.81	0.2458	0.0286	64.09	63.65
190.00	43.08	0.2302	0.0353	62.56	60.24
188.00	40.51	0.2145	0.0434	60.91	58.84
186.00	37.98	0.1982	0.0566	59.99	61.10
184.00	35.61	0.1841	NA	61.13	NA
		LCST (L_1 = L_2-V)			
182.73	34.05	0.1479	0.1479	57.97	57.97

[a] Each point given is average of several actual data points. NA = Not measured.

S solid phase
T temperature
V vapor phase

Registry No. Methane, 74-82-8; pentane, 109-66-0; octane, 111-65-9; hexane, 110-54-3; carbon dioxide, 124-38-9.

Literature Cited

(1) Hottovy, J. D.; Kohn, J. P.; Luks, K. D. *J. Chem. Eng. Data* **1981**, *26*, 135.
(2) Hottovy, J. D.; Kohn, J. P.; Luks, K. D. *J. Chem. Eng. Data* **1982**, *27*, 298.
(3) Creek, J. L.; Knobler, C. M.; Scott, R. M. *J. Chem. Phys.* **1981**, *74*, 3489.
(4) Lin, Y. N.; Chen, R. J. J.; Chappelear, P. S.; Kobayashi, R. *J. Chem. Eng. Data* **1977**, *22*, 402.
(5) Kohn, J. P. *AIChE J.* **1961**, *7*, 514.
(6) Hottovy, J. D. Ph.D. Thesis, University of Notre Dame, Notre Dame, IN, 1980.
(7) Mraw, S. C.; Hwang, S.-C.; Kobayashi, R. *J. Chem. Eng. Data* **1976**, *23*, 135.
(8) Graboski, M. S.; Daubert, T. E. *Ind. Eng. Chem. Process Des. Dev.* **1978**, *17*, 443.
(9) Graboski, M. S.; Daubert, T. E. *Ind. Eng. Chem. Process Des. Dev.* **1978**, *17*, 448.
(10) Chu, T.-C.; Chen, R. J. J.; Hcappelear, P. S.; Kobayashi, R. *J. Chem. Eng. Data* **1978**, *21*, 41.

Received for review July 8, 1982. Accepted November 22, 1982. We are grateful for the support of this work provided by the Gas Processors Association (Research Project 795), Tulsa, OK. The apparatus was assembled under research grants by the National Science Foundation.

Isentropic Compressibility of an Ideal Ternary Solution

William E. Acree, Jr.
Department of Chemistry, Kent State University, Kent, Ohio 44242

An equation is given for the isentropic compressibility of an ideal ternary solution and is used to calculate excess isentropic compressibilities of o-xylene + acetone + benzene, o-xylene + acetone + cyclohexane, and o-xylene + acetone + carbon tetrachloride mixtures. The results of these calculations indicate that the three ternary mixtures do not exhibit the large deviations from ideality as had been suggested by the earlier calculations of Prasad and Prakash.

In several recent publications appearing in this journal (*1-3*), the excess isentropic compressibility K_s^{ex} of a liquid mixture was defined as the difference between the observed isentropic compressibility and that of an ideal solution K_s^{ideal} as in eq 1.

$$K_s^{ex} = K_s - K_s^{ideal} \quad (1)$$

The isentropic compressibility of the ideal solution was represented as the mole fraction average of the isentropic compressibilities of the pure liquids $K_s^{\circ}{}_i$ (eq 2). While many

$$K_s^{ideal} = \sum_{i=1}^{N} X_i K_s^{\circ}{}_i \quad (2)$$

thermodynamic and physical properties of an ideal solution are correctly described by mole fraction averages, the isentropic compressibility is not one of these properties.

The isentropic compressibility of any solution is related to the isothermal compressibility K_t by

$$K_s = K_t(C_v/C_p) \quad (3)$$

$$K_s = -(\partial \ln V/\partial P)_S \quad (4)$$

$$K_t = -(\partial \ln V/\partial P)_T \quad (5)$$

Table I. Excess Isentropic Compressibilities of Several Ternary Mixtures

X_2	X_3	$10^{12}K_s$, cm² dyn⁻¹	K_s^{ex} eq 1 and 2	K_s^{ex} eq 1 and 9
		o-Xylene + Acetone + Benzene		
0.00	0.60	64.22	−0.59	−0.76
0.10	0.50	65.24	−1.73	−1.02
0.20	0.40	66.33	−2.80	−1.55
0.30	0.30	67.66	−3.63	−1.90
0.40	0.20	69.44	−4.01	−1.84
0.50	0.10	71.15	−4.46	−1.91
0.60	0.00	73.55	−4.22	−1.35
0.50	0.50	74.92	−2.61	−1.60
		o-Xylene + Acetone + Cyclohexane		
0.00	0.60	72.04	−1.86	−1.72
0.10	0.50	72.69	−1.85	−1.22
0.20	0.40	73.02	−2.17	−1.09
0.30	0.30	73.30	−2.54	−0.98
0.40	0.20	73.45	−3.03	−1.44
0.50	0.10	73.53	−3.60	−1.14
0.60	0.00	73.55	−4.22	−1.35
0.50	0.50	86.68	+1.58	+2.26
		o-Xylene + Acetone + Carbon Tetrachloride		
0.00	0.60	67.11	−1.65	−1.59
0.10	0.50	67.59	−2.67	−2.01
0.20	0.40	68.19	−3.57	−2.41
0.30	0.30	69.24	−4.03	−2.36
0.40	0.20	70.68	−4.09	−1.92
0.50	0.10	72.07	−4.20	−1.80
0.60	0.00	73.55	−4.22	−1.35
0.50	0.50	78.30	−2.52	−1.50

the ratio of heat capacities at constant volume and pressure, which are themselves related through

$$C_p - C_v = \alpha^2 VT/K_t \quad (6)$$

the coefficient of thermal expansion ($\alpha = (\partial \ln V/\partial T)_P$). The isothermal compressibility of an ideal solution can easily be

0021-9568/83/1728-0215$01.50/0